Journal of the Korean Association for Spatial Structures
Vol. 9, No. 4 (통권 38호), pp.49~59, December, 2009

정적해석에 의한 학교 체육관의 내진 성능 평가

Seismic Performance Evaluation of a School Gymnasium Using Static Anlysis

Shigehiro Morooka* Seita Tsuda** Makoto Ohsaki***

요 약

학교체육관과 같은 소 규모 공간구조물의 지진응답은 본래 지진동에 대한 동적응답을 시각이력해석에 의해 검증해야 하지만 통상은 정적해석에 의해 평가하고 있다. 본 연구에서는 학교 체육관의 내진성능평가를 가능하게 하는 정적해석의 진행수순을 나타내기로 한다. 지진하중은 2개의 성능 레벨 즉, 일본의 건축기준법에 정의되어 있는 레벨 1과 2에 대응하는 등가인 정적하중으로 근사한다. 또한, 재하 패턴으로서 고유모드형을 사용하는 것에 대한 중요성을 논의하고, 정적해석의 간단한 순서에 의해 최대연직방향가속도를 평가할 수 있는 것을 나타낸다. 아울러, 레벨 2의 입력에 의한 정적해석은 동적해석으로 얻어진 응답치를 과소평가하지만, 일본의 중층구조에 사용되는 "극한내력계산법"에 근사한 등가선형화 기법에 의해 레벨 2의 입력에 대한 탄소성응답이 가능하다는 것을 나타내고자 한다.

Abstract

The seismic responses of small-scale spatial frames such as school gymnasiums are usually evaluated using static analysis, although time-history analysis should be carried out to fully incorporate the dynamic responses of the structures against seismic motions. In this study, advanced static analysis procedures are presented for school gymnasiums that will improve the performance evaluation against seismic motions. The seismic loads are approximated by equivalent static loads corresponding to the two performance levels; i.e., Levels 1 and 2 defined by the Japanese building standard. The importance of utilizing the eigenmode in the load pattern is discussed. Simple static analysis procedures are presented for evaluation of maximum vertical acceleration. It is shown that the static analysis for Level 2 input significantly underestimates the responses by dynamic analysis; however, the inelastic responses for Level 2 are shown to be successfully evaluated using the equivalent linearization that is similar to the °Dmethod based on calculation of limit strength°± for building frames in Japan.

키워드 : 지진 설계, 성능레벨 설계, 학교 체육관, 등가 선형화

Keywords : Seismic design, Performance-based design, School gymnasium, Equivalent linearization

1. Introduction

In the countries prone to seismic hazards, the small-scale spatial structures such as school gymnasiums play important roles as evacuation facilities [1]. Therefore, such structure should be designed and constructed based on strict evaluation of seismic responses and performances under several levels of seismic motions [2]. However, in Japan, a school gymnasium is designed in the same manner as standard low-rise building frames using static analysis without carrying out modal analysis or time-history analysis.

It is true that we cannot demand dynamic analysis for all small-scale spatial frames, because many of them are designed and

* Dept. of Architecture, Tokai University (moro@keyaki.cc.u-tokai.ac.jp)
** Seita Tsuda Structural Engineering
*** Dept. of Architecture and Architectural Engineering, Kyoto University

constructed by the engineers who do not have enough knowledge on dynamic analysis. However, it is also true that the responses of these structures are significantly different from those of the standard building frames.

The main purpose of this paper is to present an advanced static analysis procedures for school gymnasiums that will improve the performance evaluation against seismic motions. The importance of utilizing the eigenmode in the load pattern is discussed. A simple static analysis method is presented for evaluation of maximum accelerations. Applicability of equivalent linearization method are also investigated for prediction of inelastic responses.

2. Description of Gymnasium Model and Its Seismic Performance

Seismic responses are evaluated for a typical steel gymnasium [3], as shown in Fig. 1, which is designed by slightly simplifying the frame classified as S1-type in Ref. [4]. The eaves height is 8.3 m, and the maximum height is 11.8 m. The two levels of input motions (Levels 1 and 2) specified by Notification 1461 of the Ministry of Land, Infrastructure and Transport (MLIT), Japan are considered. The responses should be within the damage limit for Level 1 motions.

For the regular building frames, the life-safety is required for Level 2 motions. However, for school gymnasiums, the serviceability as evacuation facility and enough strength for the aftershocks should be maintained for Level 2 motions as proposed in the draft of the guideline [1] for performance-based design of school gymnasiums, which demands, e.g., the following performances:

1. Maximum absolute values of the drift angles of the columns should be within the specified limit so that the nonstructural components such as the exterior walls may not be damaged.
2. Maximum values of vertical acceleration of the roof should be within the specified limit so that the nonstructural components and the hanging devices such as speakers and ceilings do not fall.
3. Maximum shear angle of the roof grid should be within the specified limit so as not to lead to any damage of roof-braces including their connections, which is very important to assure the rigidity of the roof to transmit the horizontal forces to the side frames with wall-braces.
4. Residual interstory drift angles should be small enough so that the columns and braces can have sufficient strength against the possible aftershocks and no difficulty exists for the operation of windows and entrances.

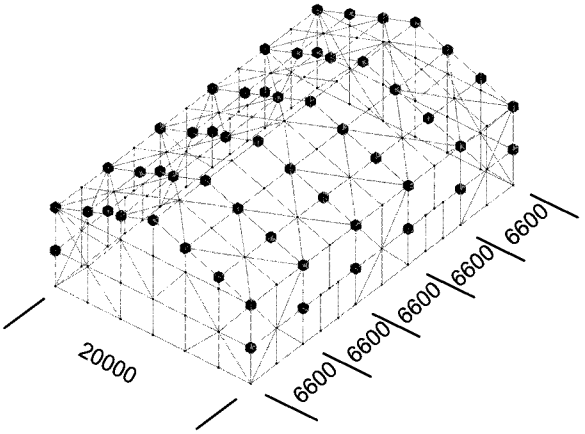

〈Fig. 1〉 A school gymnasium model

Note that the specification for the details such as connections can be found in the codes and standards for the general steel building frames. Therefore, we concentrate in this study on the responses that are specific to the small spatial frames as shown in Fig. 1. The locations of beams, columns, and braces are described in Fig. 2. Each member consists of the section as listed in Table 1. The ○ mark in Fig. 2 indicates a pin joint at the member end, where the torsional force is assumed to be transmitted. The braces V1-V3, which originally had angle sections in Ref. [3] are modeled by rectangular

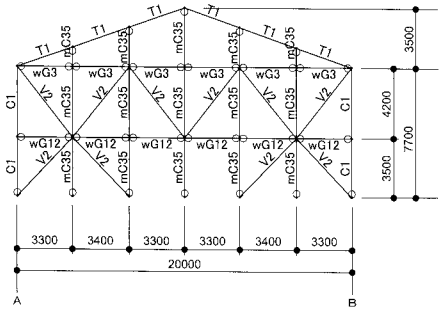

(a) Elevation in span direction (Frames(1) and (6))

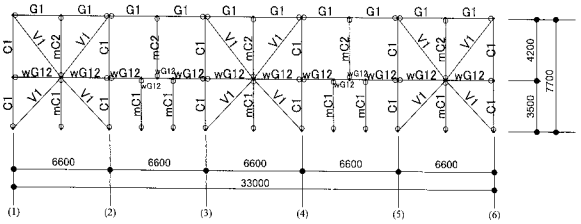

(b) Elevation in longitudinal direction (FramesA and B)

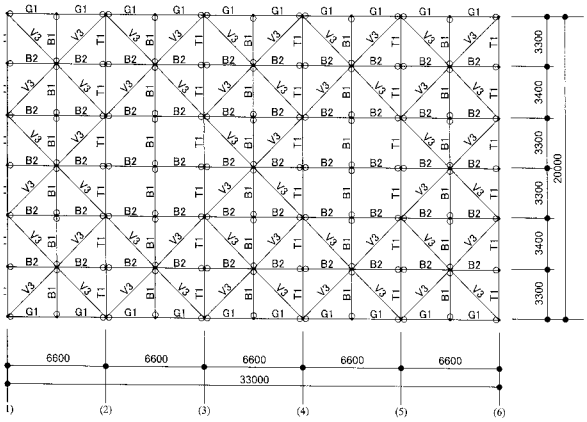

(c) Roof Plan

〈Fig. 2〉 Lacations of the beams, columns, and braces

solid sections (plates) with the same cross-sectional areas. Furthermore, the latticed beam G1 in Ref. [3] is replaced by a wide-flange section with similar geometry. Note that the height of each column in Fig. 2 is 7.7 m, which is smaller than the eaves height 8.3 m, because the centerlines of members are drawn in Fig. 2.

The construction site of the gymnasium is supposed to be in a region of heavy snow in Japan. The building area is 679.96 m2 which is equal to the floor area. The number of floors is regarded to be 1 based on the Japanese building standard. The materials are steel for the beams, columns, and braces, and RC for the independent bases.

〈Table 1〉 Member sections.

	Original	Modified
T1	H-692x300x13x20	
G1	2[-300x90x9x13	H-594x302x14x23
B1	H-175x90x5x8	
B2	H-300x150x6.5x9	
wG1,2	H-300x150x6.5x9	
wG3	H-150x100x6x9	H-148x100x6x9
C1	H-594x302x14x23	
mC1	H-150x100x6x9	H-148x100x6x9
mC2	H-150x100x6x9	H-148x100x6x9
mC3-5	H-300x150x6.5x9	

Each frame in the span direction is a rigidly-jointed moment frame with pin supports at the bases. Frames (1) and (6) in both sides of the span-direction have braces, and the forces on the roof are transmitted to the side frames through the roof braces. The frames in the longitudinal direction are pin-jointed braced frames, where all the horizontal loads are resisted by the braces.

The steel materials are SS400 for the steel beams, columns, and braces including welding. The weights of the roof are 294 N/m^2 for the self-weight, 588 N/m2 for the service loads, and 1029 N/m^2 for the snow loads. The weights for the walls are 637 N/m^2 for the ALC panel, and 294 N/m^2 for the columns including the nonstructural columns. Therefore, the total load for evaluation of seismic responses is 294 + 588 + 1029 = 1911 N/m^2 for the roof, and 637 + 294 = 931 N/m^2 for the wall. The total weight of the structure is 203,000 kgf (1990 kN).

The locations of 54 concentrated nodal masses are shown in Fig. 1; i.e., each of 6 frames in span direction has 9 masses. Note that the values of the masses are different depending on the covering areas and the mass per unit area of the nodes. The mass (weight) of the wall higher than 3.5/2 = 1.75 m from GL is included in the concentrated masses on the walls in Frames (1) and (6). However, since there is no mass on the side walls in Frames (A)

and (B) in the span direction, all masses of the wall are included in the concentrated mass located on the roof.

3. Results of Eigenvalue Analysis

Eigenvalue analysis has been carried out for two cases, where the compressive stiffness of the brace is considered and neglected, respectively. In the latter case, the stiffnesses of all braces are scaled to half for the eigenvalue analysis. If the compressive stiffness of braces is considered, the 1st mode vibrates in the span direction, as shown in Fig. 3, where the period is 0.364 sec., and the effective mass ratio is 84.80% for horizontal input; i.e., the first mode is dominant in vibration against seismic excitation in span direction. The 1st period and the corresponding effective mass ratio are 0.464 and 84.40%, respectively, if the compressive stiffness of braces is neglected.

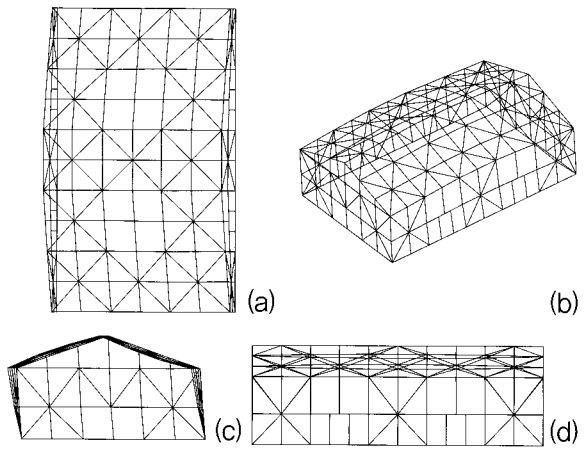

〈Fig. 3〉 1st eigenmode; (a): plane, (b) bird-eye's view, (c), (d): elevation.

4. Static and Dynamic Seismic Loads

The gravity loads are applied neglecting the braces prior to the analysis against seismic loads, because braces are attached after constructing the frames. The braces are assumed to transmit tensile forces only due to their very large slenderness ratios. The following three patterns are considered for the seismic loads, where the loads are distributed to 54 nodes with concentrated masses defined in Fig. 1. In this paper, the responses in the span direction are presented due to the limitation in the volume of the paper. Analysis is carried out using the software package MIDAS/Gen [5].

Static load SA:

Let b = (11.8+8.3)/2 = 10.0 m denote the average height of the structure. Then, based on the Japanese code, the first period is approximately computed as T = 0.03b = 0.30 sec., and the coefficient Rt that defines the amplification factor of acceleration is 1.0. Therefore, the total seismic load for Level 1, denoted by SA-1 corresponding to the base shear coefficient C0 = 0.2, is 1990×0.20 = 398 kN.

Static load SB:

The seismic loads are applied at the 54 nodes proportionally to the 1st mode. The magnitude of loads for Level 1, denoted by SB-1, is adjusted so that the total load is equal to 1990× 0.20 = 398 kN corresponding to the base shear coefficient C0 = 0.2.

Dynamic load D:

Seismic responses are computed by time-history analysis. The modal damping coefficients are proportional to the frequency with 0.02 for the 1st mode. A set of 15 artificial seismic motions are generated to be compatible to the design acceleration response spectrum for 5% damping specified by Notification 1461 of MLIT, Japan. The amplification factor for the ground of second rank is used as defined in Notification 1457 of MLIT. The target design acceleration response spectrum for Level 1 motion (D-1) is plotted in dotted lines in Fig. 4 together with the response spectrum of one of

the artificial motions. The level is scaled by 5 for Level 2 motion (D-2). The maximum absolute value of each response is evaluated during the duration of 20 seconds for each input motion.

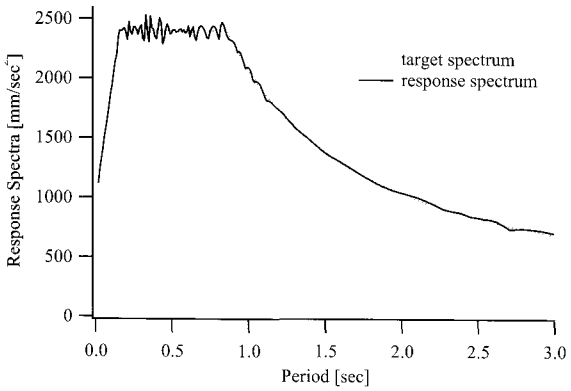

〈Fig. 4〉 Acceleration response spectrum for Level 1 motion with 5% damping.

5. Responses to Level 1 Motions

Based on the performance requirements in Ref. [6], no damage should be expected for the Level 1 input. The maximum responses of acceleration, relative displacement, reaction force, and interstory drift angle obtained by SA-1, SB-1, and D-1 are compared. The values in the parentheses ( ) in the following tables are the ratios to the values for SA-1. The response accelerations and displacements are evaluated at the points indicated by ● in Fig. 5. The height of each evaluation point is denoted by H, and H = 11200 corresponds to the top node.

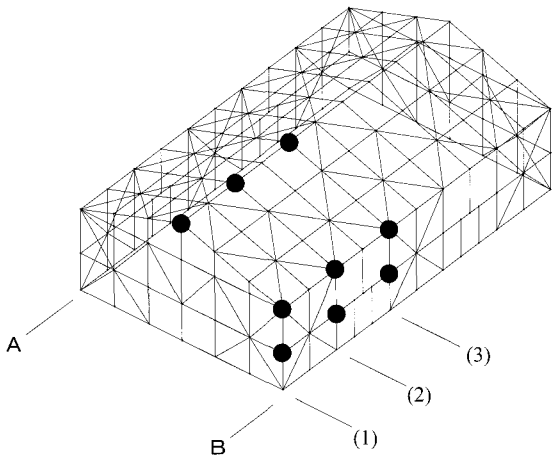

〈Fig. 5〉 Evaluation points of acceleration and displacement.

Maximum accelerations

The acceleration responses in span direction are listed in Table 2. Let G denote the acceleration of gravity. The accelerations for SA-1 are not shown, because they are 0.2G for all nodes by definition of the load. The accelerations for SB-1 are evaluated by dividing the nodal load by the nodal weight and multiplying G. Therefore, the nodal accelerations are proportional to the corresponding components of the 1st mode.

At the top of the frame, the accelerations by SB-1 for Frames (1) and (3) are 43% smaller and 48% larger, respectively, than that by SA-1 with uniform accelerations. Therefore, the use of the static loads proportional to the dominant mode is very important for evaluation of maximum accelerations. The mean values of maximum responses to 15 motions of Level 1 (D-1) are also listed in Table 2, where the values in the parentheses [ ] are the standard deviation; e.g., the mean maximum acceleration at the top of Frame (3) is 3760 and the standard deviation is 364, which are divided by the maximum response for SA-1 to obtain the ratios 1.918 and 0.186, respectively. It is also seen from Table 2 that the dynamic responses by D-1 may be significantly larger than the static responses by SB-1 at the roof nodes in Frames (2) and (3).

Maximum displacements

The maximum displacements are listed in Table 3. The static load SA-1 with uniform acceleration also underestimates the displacement at the top of Frame (3); however, the difference is smaller than the acceleration response, because the displacements **U** are computed from the loads **P** and the stiffness matrix **K** using the stiffness equations **P** = **KU**, which reduces the effect of differences in **P**. The

〈Table 2〉 Maximum accelerations (mm/sec^2) for Level 1.

Frame		(1)	(2)	(3)
SB-1	H = 11200	1117 (0.57)	2038 (1.04)	2901 (1.48)
	7700	1078 (0.55)	2038 (1.04)	2901 (1.48)
	3500	529 (0.27)	1098 (0.56)	1548 (0.79)
D-1	11200	1742[185]	2768[273]	3760[364]
		(0.889[0.094])	(1.412[0.14])	(1.918[0.186])
	7700	1736[194])	2803[275]	3774[345]
		(0.886[0.099])	(1.43[0.14])	1.926[0.176])
	3500	1384[113])	1689[133]	2148[219]
		(0.706[0.057])	(0.862[0.068])	(1.096[0.112])

differences between the static and dynamic responses are also smaller than those for the accelerations.

〈Table 3〉 Maximum displacements (mm) for Level 1.

Frame		(1)	(2)	(3)
SA-1	H = 11200	6.26	10.88	14.01
	7700	6.18	10.85	14
	3500	3.25	5.91	7.62
SB-1	11200	6.23 (1.00)	12.08 (1.11)	17.01 (1.21)
	7700	6.14 (0.99)	12.03 (1.11)	16.99 (1.21)
	3500	3.19 (0.98)	6.47 (1.09)	9.16 (1.20)
D-1	11200	7.940[0.78] (1.27[0.12])	15.43[1.52] (1.42[0.14])	21.62[2.12] (1.54[0.15])
	7700	7.75[0.78] (1.25[0.13])	15.39[1.52] (1.42[0.14])	21.58[2.13] (1.54[0.15])
	3500	4.06[0.4] (1.25[0.12])	8.27[0.81] (1.4[0.14])	11.59[1.14] (1.52[0.15])

Maximum drift/shear angles

The maximum drift angles of wall and shear angles of roof are listed in Table 4. Note that the values of the roof are computed from the displacements at the center and side that are projected to the horizontal plane assuming that the inclination of the roof is sufficiently small. As is seen, the static analyses, especially SA-1, significantly underestimate the maximum drift/shear angles by obtained dynamic analysis.

〈Table 4〉 Maximum drift angles (×10-3 rad.) for Level 1.

	Roof	Wall
SA-1	0.700	0.803
SB-1	0.887 (1.27)	0.797 (0.99)
D-1	1.158[0.123] (1.65[0.18])	1.999[0.204] (2.49[0.25])

Maximum reaction forces

The maximum reaction forces of each frame and the total frame are listed in Table 5. The reaction force of Frame (1) is larger than those of Frames (2) and (3), because Frame (1) has larger stiffness than the other frames. However, the reaction force of Frame (3) by SB-1 is larger than that by SA-1, because Frame (3) has larger acceleration than Frame (1) for SB-1. It is also observed from Table 5 that the reaction forces by dynamic analysis D-1 are larger than those of static analyses.

〈Table 5〉 Maximum reaction forces (kN) for Level 1.

	Frame (1)	Frame (2)	Frame (3)	Total
SA-1	150	22	27	398
SB-1	147 (0.98)	22 (1.00)	31 (1.15)	398 (1.00)
D-1	178.3[22.7] (1.19[0.15])	26[3.2] (1.18[0.15])	36.2[4.4] (1.34[0.16])	481 (1.21)

Vertical accelerations

The vertical accelerations should be evaluated to investigate the forces applied to the hanging equipments such as speakers and lights. Since dynamic analysis is not carried out in the practical design process, it is important to present a simple method for estimating the vertical acceleration using static analysis. For this purpose, the pseudo-accelerations are computed by multiplying the square of the 1st circular frequency to the vertical displacements evaluated by SA-1 and SB-1, respectively. The

〈Table 6〉 Maximum reaction forces (kN) for Level 1.

Node location		Vertical disp. δ (mm)		Vertical acc. $\delta \cdot \omega^2$ (mm/sec^2)		Vertical acc. (mm/sec^2)
Frame	Line	SA-1	SB-1	SA-1	SB-1	D-1
(2)	a	0.06	0.13	11	24	254[16]
(2)	b	1.29	1.50	236	275	581[76]
(2)	c	1.50	1.72	275	315	580[67]
(3)	a	0.07	0.07	13	13	202[27]
(3)	b	1.51	1.97	277	361	656[49]
(3)	c	1.84	2.35	337	430	682[59]

results are shown in Table 6 for the points indicated by ● in Fig. 6.

Since the static deformation is almost antisymmetric with respect to the vertical plane containing line a' in Fig. 6, the vertical accelerations at the top nodes are very small. The responses by SA-1 are smaller than those by SB-1 also for the vertical acceleration. It is also seen from Table 6 that the pseudo-accelerations by static analysis are significantly smaller than those by dynamic analysis, because the effect of higher modes, which do not have clear antisymmetric properties, is neglected in the static analysis; hence, the dynamic responses have moderately large values at the nodes in line a'.

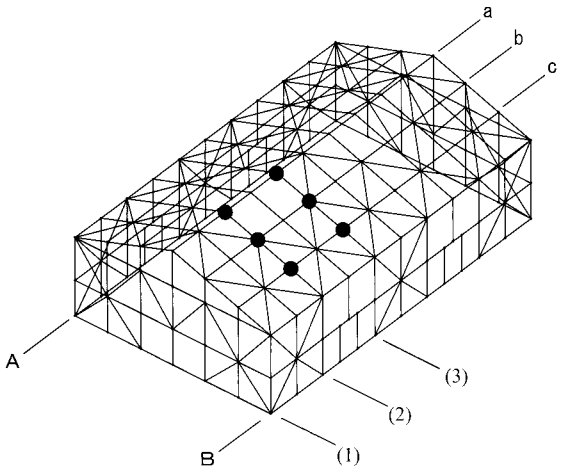

〈Fig. 6〉 Evaluation points of vertical acceleration

6. Responses for Level 2 Motions

6.1 Static analysis

Pushover analyses are carried out for the patterns SA-2 and SB-2 corresponding to Level 2 input. The yield stress of steel is 235×1.1 N/mm2, and the stiffness after yielding is 1% of the initial stiffness. The result before the base shear coefficient reaches 1.2 is shown in Fig. 7, where the vertical axis is the total load, and the horizontal axis is the displacement at the point indicated by ● in Fig. 8.

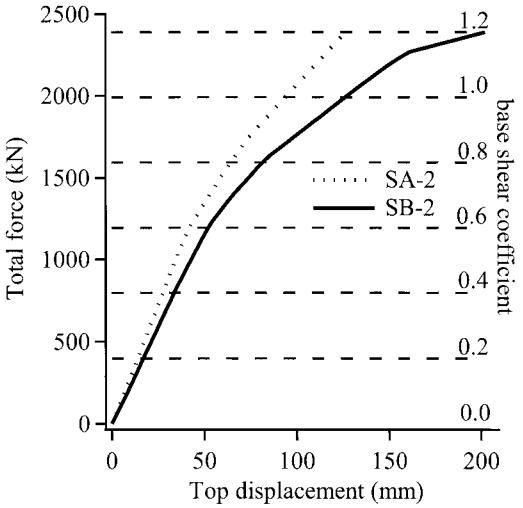

〈Fig. 7〉 Results of pushover analysis.

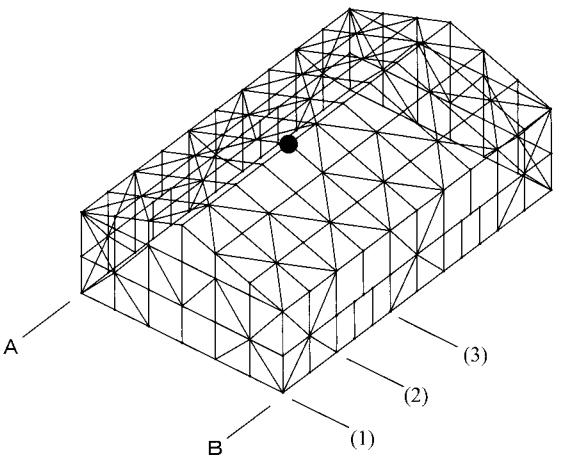

〈Fig. 8〉 Evaluation point of displacements (indicated by ●).

The braces in the side frames start to yield at the base shear equal to 1300 kN. The beams and columns of the frames have enough stiffness after the first yielding of the brace,

and the columns at the corners yield when the base shear is equal to 2300 kN for SB-2, whereas those columns do not yield for SA-2. Furthermore, SB-2 leads to larger roof displacement than SA-2, because the former has larger loads than the latter at the top. Therefore, the eigenmodes should be used for defining the load pattern for static pushover analysis for Level-2 input.

Since the braces of this frame have moderately large slenderness rations, and are categorized as BB-rank in the Japanese code, the value of Ds' that defines the maximum base shear coefficient for the plastic limit analysis is 0.4. As is seen from Fig. 7, the response against the horizontal load of the total weight 1990 kN scaled by 0.4; i.e., 800 kN, are in the elastic range, and are equal to the twice of the responses for Level 1 input with C0 = 0.2.

Hence, the maximum displacement for limit analysis at the top of Frame (3) for SA-2, which is usually used in practical design process, is 14.01?2 = 28.02 mm.

6.2 Dynamic analysis

The seismic motions for Level 1 are scaled by 5 to obtain the motions for Level 2. The yield stress is assumed to be 235×1.1 N/mm2, and the hardening ratio is 0.01 also for dynamic analysis. The braces are modeled by a slip-type bilinear force-elongation relation. The yield forces are 310 kN for wall-braces, and 194 kN for roof-braces. The normal bilinear model is used for bending along the strong axis of the beams and columns, and interaction between bending moment and axial force in evaluation of bending strength is not considered. For example, the yield moments are 1308 kNm for column C1, and 1422 kNm for beam T1.

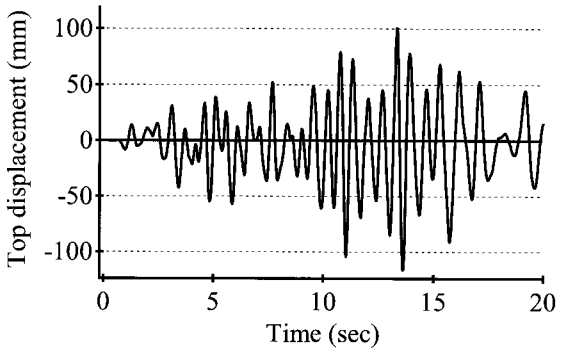

〈Fig. 9〉 Time-history of displacement of the top node.

The time-history of the displacement of the top node indicated in Fig. 8 for one of the 15 motions is plotted in Fig. 9.

The mean maximum values and standard deviations of the reaction forces of Frames (1), (2) and (3) are listed in Table 7. If we assume that the three frames have the maximum reaction forces at the same time instance, then the mean maximum value of the total reaction force is (597.5+160.2+186.6) ×2 = 1888.6 kN, which approximately corresponds to the base shear coefficient C0 = 1.0 for the Level 2 input. Therefore, it can be assumed that the 1st mode dominates in the response and the phase differences in the vibrations of three frames can be neglected.

〈Table 7〉 Mean values and standard deviations of maximum reaction forces (kN) for Level 2.

	Frame(1)	Frame(2)	Frame(3)
D-2	597.5[30.2]	160.2[18.8]	186.6[22.3]

The maximum displacements are listed in Table 8. As is seen, the responses are between 5 times and 9 times as large as those for Level 1 input in Table 3. The maximum shear angle of the roof computed from the displacements at the center and side is 1/112, and the maximum interstory drift angle of the wall is 1/167, which are about 7 times to 9 times as large as the responses for D-1. Therefore, static analysis with the reduction factor Ds = 0.4 significantly underestimates, as shown in Sec. 6.1, the responses for Level 2 input.

〈Table 8〉 Mean values and standard deviations of maximum displacements (mm) for Level 2.

	Frame (1)	Frame (2)	Frame (3)
H = 11,200	43.6 [7.1]	89.9 [12.1]	106.5 [12.1]
H = 7,700	43.1 [7.1]	89.8 [11.8]	106.3 [12.1]
H = 3,500	26.2 [4.3]	48.2 [6.0]	57.2 [6.5]

The maximum vertical accelerations are listed in Table 9. Note that the vertical accelerations of the top node have moderately large values, because the antisymmetry of the deformation is broken due to partial plastification.

〈Table 9〉 Mean values and standard deviations of maximum vertical accelerations (mm/sec2).

Node	Frame (2)	Frame (3)
a	2198 [304]	1527 [366]
b	6763 [924]	3663 [447]
c	6428 [804]	3654 [455]

6.3 Response evaluation by equivalent linearization

It is well known that the inelastic responses of building frames can be evaluated with good accuracy using the equivalent linearization, e.g., the capacity spectrum approach. However, applicability of this method is not verified for school gymnasiums consisting of very slender steel beams, columns, and braces. Therefore, we compare the results of two types of linearization methods with those of dynamic analysis under Level-2 motions. The two methods use different definitions of the equivalent damping ratio; however, any definition can be used for each method.

The first method is similar to the "Method based on calculation of limit strength" that does not compute eigenmodes and the load pattern is SA-2. The second method utilizes eigenvalue analysis considering the compressive stiffness of the braces, i.e., the load pattern is SB-2, although the model without the compressive stiffness can also be used.

The common parameter values and definitions for the two methods are as follows:

* Damping ratio for initial elastic state is h = 0.02.
* The representative displacement at the response evaluation point in Fig. 8 and base shear coefficient at yielding obtained by pushover analysis in Sec. 6.1 are 52 mm and 1200 kN, respectively.
* Reduction factor of the response spectrum is given as

$F_h = \frac{1.5}{1+10h_e}$, h_e : equivalent damping ratio

* Equivalent period is computed from the displacement response spectrum S_D and the acceleration response spectrum S_A as

$T_e = 2\pi\sqrt{S_D / S_A}$

Method 1: without eigenvalue analysis

Let m_j and δ_i denote the mass and displacement of node i at a step of the pushover analysis. The capacity spectrum is computed by

$$M_e = \frac{\left(\sum m_i\delta_i\right)^2}{\sum m_i\delta_i^2},\quad S_D = \frac{\sum m_i\delta_i^2}{\sum m_i\delta_i},\quad S_A = Q/M_e,$$

where Q is the base shear and M_e is the equivalent mass.

Let μ denote the plasticity factor obtained by dividing the representative displacement by the yield displacement 52 mm. We compute the equivalent damping ratio h_e as

$$h_e = h + \gamma\left(1 - \frac{1}{\sqrt{\mu}}\right)$$

where γ=0.2 is used [7]; however, it is very difficult to assign an appropriate value of the parameter γ for the structure which resists the horizontal loads mainly by braces that are prone to buckling.

Method 2: with eigenvalue analysis [6,8]

Let δ and ϕ_U denote the displacement at the point in Fig. 8 and the corresponding component of the 1st mode. The participation factor for the 1st mode is denoted by β. Then the capacity spectrum is computed as

$$S_D = \delta/(\beta\phi_U),\quad S_A = Q/M_e$$

and the equivalent damping ratio h_e is computed from

$$h_e = h + \kappa\frac{2(\eta-1)(1-\alpha)}{\pi\eta[1+\alpha(\eta-1)]}$$

where 0.33 for the smallest ductility is given for κ [8,9]. Note that this formula is used mainly for RC structures; therefore, the applicability of this equation is not guaranteed.

For the structure under consideration, the effective mass ratio R_e is 0.840, and the participation factor β is 0.417 for the 1st mode. The roof-displacement component ϕ_U of the 1st mode is 3.02, and the hardening coefficient obtained by the pushover curve in Fig. 7 is 0.404.

Results of analysis

The analysis results are summarized in Table 10. The capacity spectrum (pushover curve) for Method 2 is plotted in solid line Fig. 10, where the demand spectrum at the final state are plotted in the dotted horizontal line. The dashed curve indicates the path of the evaluation point that finally coincided with the intersection of the capacity and demand spectra. As is seen from Table 10, the maximum representative displacements computed by the equivalent linearization agree with the results of the dynamic analysis with good accuracy. However, it should be noted that the results significantly depend on the parameter values for the equivalent damping ratios.

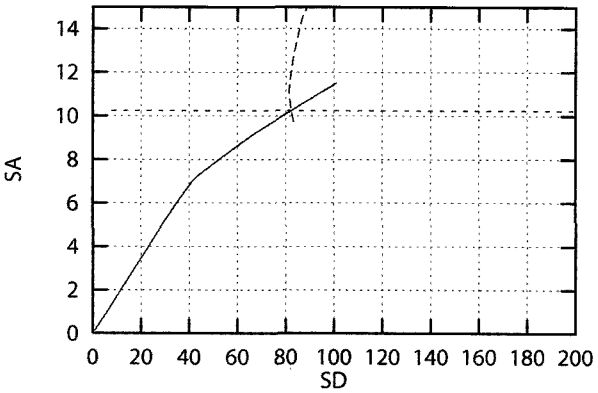

〈Fig. 10〉 Capacity spectrum (solid line) and demand spectrum (dotted line) for Method 2.

7. Conclusions

Advanced static analysis procedures have been presented for school gymnasiums to improve the accuracy of performance evaluation against seismic motions. The conclusions drawn from this study is summarized as follows:

〈Table 10〉 Results by equivalent linearization

	Method 1	Method 2
δ(mm)	100	110
F_h	0.853	0.906
h_e	0.076	0.066
μ	1.92	2.12
S_A (m/sec^2)	10.2	10.9
S_D (mm)	82	88
T_e	0.563	0.565

1. The use of the static loads based on nodal accelerations proportional to the dominant mode is very important for evaluation of maximum horizontal accelerations for Level 1 motions. Therefore, eigenvalue analysis is indispensable for accurate evaluation of responses.
2. Static analysis for Level 1 and 2 motions may significantly underestimate the mean-maximum responses obtained by dynamic analysis.
3. Maximum response accelerations can be evaluated using the dominant eigenmode and acceleration response spectrum. However, higher modes should be incorporated for evaluating the vertical responses at the top node.
4. Good approximate responses may be obtained by an equivalent linearization method, although the results strongly depend on the definition of equivalent damping ratio.

Acknowledgements

This study is a part of work in Sub-committee for Seismic Design, Committee for Shell and Spatial Structures, Architectural Institute of Japan (Chairman: M. Ohsaki, Kyoto University, 2004-2008). The authors are grateful for the collaboration of the committee members.

References

1. Guideline for Performance-Based Design of School Gymnasiums (Draft), Sub-committee for Seismic Design, Committee for Shell and Spatial Structures, Architectural

Institute of Japan, 2008. (in Japanese)
2. S. Mahin, J. Malley and R. Hamburger, Overview of the FEMA/SAC program for reduction of earthquake hazards in steel moment frame structures, J. Const. Steel Res., Vol. 58, pp. 511-528, 2002.
3. The Kozai Club, Exsercises of Design of Steel Structures, 3rd Ed., Gihoudo, 1986. (in Japanese)
4. Guideline for Performance Evaluation of Gymnasiums, MEXT, Japan, 2006. (in Japanese)
5. http://www.midasit.com/
6. ATC. ATC-40 Seismic Evaluation and Retrofit of Concrete Buildings. Applied Technology Council, Redwood City, CA, 1996.
7. Building Research Institute, Ministry of Land Infrastructure, Transportation and Tourism (Ed.), Technical Background of Structural Regulations of Revised Building Standard Law, Gyousei, pp. 40-45, 2005. (in Japanese)
8. A. K. Chopra and R. K. Goel. Capacity-demand-diagram method for estimating seismic deformations of inelastic structures: SDF systems. Report No. PEER-1999/02, Pacific Earthquake Engineering Research Center, University of California, Berkeley, April 1999.
9. S. Takeuchi, S. Otani and H. Shiohara, The effect of equivalent viscous damping ratio estimation on capacity spectrum method, Proc. Annual Meeting, B2, pp. 455-456, 2000. (in Japanese)

접수일자 : 2009년 3월 31일
심사완료일자 : 2009년 6월 1일
게재확정일자 : 2009년 10월 23일